

ADJOINED NETWORKS: A TRAINING PARADIGM WITH APPLICATIONS TO NETWORK COMPRESSION

Utkarsh Nath¹, Shrinu Kushagra², Yingzhen Yang¹

Arizona State University¹, University of Waterloo²

{unath, yyang409}@asu.edu, skushagra@waterloo.edu

ABSTRACT

Compressing deep neural networks while maintaining accuracy is important when we want to deploy large, powerful models in production and/or edge devices. One common technique used to achieve this goal is knowledge distillation. Typically, the output of a static pre-defined teacher (a large base network) is used as soft labels to train and transfer information to a student (or smaller) network. In this paper, we introduce *Adjoined Networks*, or AN, a learning paradigm that trains both the original base network and the smaller compressed network together. In our training approach, the parameters of the smaller network are shared across both the base and the compressed networks. Using our training paradigm, we can simultaneously compress (the student network) and regularize (the teacher network) any architecture. In this paper, we focus on popular CNN-based architectures used for computer vision tasks. We conduct an extensive experimental evaluation of our training paradigm on various large-scale datasets. Using ResNet-50 as the base network, AN achieves 71.8% top-1 accuracy with only 1.8M parameters and 1.6 GFLOPs on the ImageNet data-set. We further propose Differentiable Adjoined Networks (DAN), a training paradigm that augments AN by using neural architecture search to jointly learn both the width and the weights for each layer of the smaller network. DAN achieves ResNet-50 level accuracy on ImageNet with $3.8\times$ fewer parameters and $2.2\times$ fewer FLOPs.

1 INTRODUCTION

Deep Neural Networks (DNNs) have achieved state-of-the-art performance on many tasks such as classification, object detection and image segmentation. However, the large number of parameters often required to achieve the performance makes it difficult to deploy them at the edge (like on mobile phones, IoT and embedded devices, etc). Unlike cloud servers, these edge devices are constrained in terms of memory, compute, and energy resources. A large network performs a lot of computations, consumes more energy, and is difficult to transport and update. A large network also has a high prediction time per image. This is a constraint when real-time inference is needed. Thus, compressing neural networks while maintaining accuracy and improving inference time has received significant attention in the last few years. Popular techniques for network compression include pruning and knowledge distillation.

Pruning methods remove parameters (or weights) of overparameterized DNNs based on some pre-defined criteria. For example, Han et al. (2015) removes weights whose absolute value

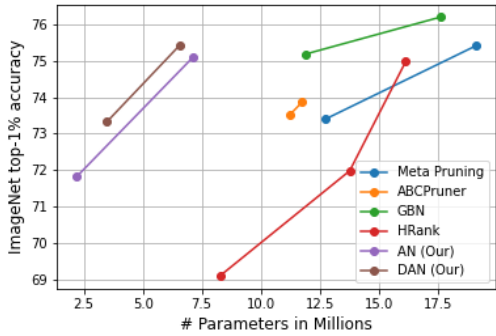


Figure 1: Top-1 accuracy of various structured pruning methods (by compressing the ResNet-50 or ResNet-100 architecture) on the ImageNet dataset plotted against the number of parameters in the model. Our methods, Adjoined Networks (AN), and Differentiable Adjoined Networks (DAN) achieve similar accuracy as compared against current SOTA pruning methods but with fewer (in many cases $2\times$ fewer) parameters.

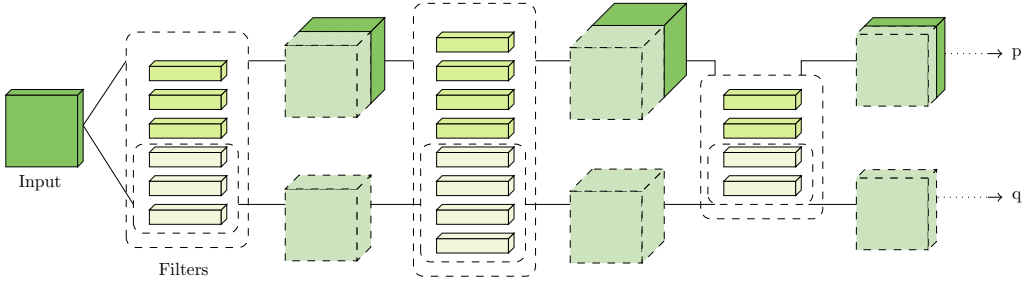


Figure 2: Training paradigm based on adjoined networks. The original and the compressed version of the network are trained together with the parameters of the smaller network shared across both. The network outputs two probability vectors p (original network) and q (smaller network).

is smaller than a threshold. While weight pruning methods are successful at reducing the number of parameters of the network, they often work by creating spares tensors that may require special hardware Han et al. (2016) or special software Park et al. (2017) to provide inference time speed-ups. These methods are also known as *unstructured pruning* and has been extensively studied in Han et al. (2015); Zhu & Gupta (2017); Gale et al. (2019); Kusupati et al. (2020); Evci et al. (2021). To overcome this limitation, channel pruning Liu et al. (2017) and filter pruning Li et al. (2016) techniques are used. These *structured pruning* methods work by removing entire convolution channels or sometimes even filters based on some pre-defined criteria and can often provide significant improvement in inference times. In this paper, we show that our algorithm, Adjoined Networks or AN, achieves accuracy similar to the current state-of-the-art structured pruning methods but uses a significantly lower number of parameters and FLOPs (Fig 1).

The AN training paradigm works as follows. A given input image X is processed by two networks, the larger network (or the base network) and the smaller network (or the compressed network). The base network outputs a probability vector p and the compressed network outputs a probability vector q . This setup is similar to the student-teacher training used in Knowledge Distillation Hinton et al. (2015) where the base network (or the teacher) is used to train the compressed network (or the student). However, there are two very important distinctions. (1) In knowledge distillation, the parameters of the base (or larger or teacher) network are fixed and the output of the base network is used as a "soft label" to train the compressed (or smaller or student) network. In the paradigm of the adjoined network, both the base and the compressed network are trained together. The output of the base network influences the compressed network and vice-versa. (2) The parameters of the compressed network are shared across both the smaller and larger networks (Fig. 2). We train the two networks using a novel time-dependent loss function called *adjoined loss*. An additional benefit of training the two networks together is that the smaller network can have a regularizing effect on the larger network. In our experiments (Section 7), we see that on many datasets and for many architectures, the base network trained in the adjoined fashion has greater prediction accuracy than the standard situation when the base network was trained alone. We also provide theoretical justification for this observation in Section 6. The details of our design, the loss function and how it supports fast inference are discussed in Section 3.

As discussed in the previous paragraph, in the AN training paradigm, all the parameters of the smaller network are shared across both the smaller and larger network. Our compression architecture design involves selecting and tuning a hyper-parameter α , the size (or the number of parameters in each convolution layer) of the smaller network as compared against the larger base network. In our experiments (Section 7) with the AN paradigm, we found that choosing a value of $\alpha = 1/4$ or $1/2$ as a global (same across all the layers of the network) constant typically worked well. To get more boost in compression performance, we propose the framework of Differentiable Adjoined Network (DAN). DAN uses techniques from Neural Architecture Search (NAS) to further optimize and choose the right value of α at each layer of our compressed model. The details of DAN are discussed in Section 5.

Below are the main contributions of this work.

1. We propose a novel training paradigm based on *Adjoined Networks* or AN, that can compress any CNN based neural architecture. This involves adjoined training where the original network and the smaller network are trained together. This has twin benefits of compression and regularization whereby the larger network (or teacher) transfers information and helps compress the smaller network while the smaller network helps regularize the larger teacher network.
2. We further propose *Differentiable Adjoined Networks*, or DAN, that adjointly learns some of the hyper-parameters of the smaller network including the number of filters in each layer of the smaller network.
3. We conducted an exhaustive experimental evaluation of our method and compared it against several state-of-the-art methods on datasets such as ImageNet Russakovsky et al. (2015) and CIFAR-100 Krizhevsky et al. (2009). We consider different architectures such as ResNet-50, ResNet-18 and DenseNet-121. On ImageNet, using adjoined training paradigm, we can compress ResNet-50 by $4\times$ with $2\times$ FLOPs reduction while achieving 75.1% accuracy. Moreover, the base network gains 0.7% in accuracy when compared against the same network trained in the standard (non-adjoined) fashion. We further increase the accuracy of the compressed model to 75.7% by augmenting our approach with architecture search (DAN), clearly showing that it is *better* to train the networks *together*.

The paper is organized as follows. In Section 2, we discuss some of the other methods that are related to the discussions in the paper. In Section 3, we provide details of the architecture for adjoined networks and the loss function. In Section 4, we show how training both the base and compressed network together provides compression (for the smaller network) as well as regularization (for the larger network). In Section 5, we combine AN with neural architecture search and introduce Differentiable Adjoined Networks (or DAN). In Section 6, we provide strong theoretical guarantees on the regularization behaviour of adjoined training. In Section 7, we provide the details of our experimental results.

2 RELATED WORK

In this section, we discuss various techniques used to design efficient neural networks in terms of size and FLOPs. We also compare our approach to other similar approaches and ideas in the literature.

Knowledge Distillation is the transfer of knowledge from a cumbersome model to a small model. Hinton et al. (2015) proposed teacher student model, where soft targets from the teacher are used to train the student model. This forces the student to generalize in the same manner as the teacher. Various knowledge transfer methods have been proposed recently. Romero et al. (2015) used intermediate layer’s information from teacher model to train thinner and deeper student model. Peng et al. (2019) proposes to use instance level correlation congruence instead of just using instance congruence between the teacher and student. Ahn et al. (2019) tried to maximize the mutual information between teacher and student models using variational information maximization. Park et al. (2019) aims at transferring structural knowledge from teacher to student. Kim et al. (2020) argues that directly transferring a teacher’s knowledge to a student is difficult due to inherent differences in structure, layers, channels, etc., therefore, they paraphrase the output of the teacher in an unsupervised manner making it easier for the student to understand. Most of these methods use a trained teacher model to train a student model. In contrast in this work, we train both the teacher and the student together from scratch. In recent work, Zhang et al. (2018), rather than using a teacher to train a student, they let a cohort of students train together using a distillation loss function. In this paper, we consider a teacher and a student together rather than using a pre-trained teacher. We also use a novel time-dependent loss function. Moreover, we also provide theoretical guarantees on the efficacy of our approach. We have compared our AN with various knowledge distillation methods in the experiments section.

Pruning techniques aim to achieve network compression by removing parameters or weights from a network while still maintaining accuracy. These techniques can be broadly classified into two categories; unstructured and structured. Unstructured pruning methods are generic and do not take network architecture (channel, filters) into account. These methods induce sparsity based on some pre-defined criteria and often achieve a state-of-the-art reduction in the number of parameters. However, one drawback of these methods is that they are often unable to provide inference time

speed-ups on commodity hardware due to their unstructured nature. Unstructured sparsity has been extensively studied in Han et al. (2015); Zhu & Gupta (2017); Gale et al. (2019); Kusupati et al. (2020); Evci et al. (2021). Structured pruning aims to address the issue of inference time speed-up by taking network architecture into account. As an example, for CNN architectures, these methods try to remove entire channels or filters, or blocks. This ensures that the reduction in the number of parameters also translates to a reduction in inference time on commodity hardware. For example, ABCPruner Lin et al. (2020b) decides the convolution filters to be removed in each layer using an artificial bee colony algorithm. Lin et al. (2020a) prunes filters with low-rank feature maps. You et al. (2019) uses Taylor expansion to estimate the change in the loss function by removing a particular filter, and finally removes the filters with max change. The AN compression technique proposed in this paper can also be thought of as a structured pruning method where the architecture choice at the start of training fixes the convolution filters to be pruned and the amount of pruning at each layer. Another related work is of Slimmable Networks Yu et al. (2018). Here different networks (or architectures) are *switched on* one at a time and trained using the standard cross-entropy loss function. By contrast, in this work, both the networks are trained together at the same time using a novel loss function (adjoined-loss). We have compared our work with Slimmable Networks in Table 1.

Neural Architecture Search (NAS) is a technique that automatically designs neural architecture without human intervention. The best architecture could be found by training all architectures in the given search space from scratch to convergence but this is computationally impractical. Earlier studies in NAS were based on RL Zoph & Le (2017); Tan et al. (2019) and EA Real et al. (2017), however, they required lots of computation resources. Most recent studies Liu et al. (2019a); Cai et al. (2019); Wu et al. (2019) encode architectures as a weight sharing a super-net and optimize the weights using gradient descent. A recent study Meta Pruning Liu et al. (2019b) searches over the number of channels in each layer. It generates weights for all candidates and then selects the architecture with the highest validation accuracy. A lot of these techniques focus on designing compact architecture from scratch. In this paper, we use architecture search to help guide the choice of architecture for compression, that is, what fraction of filters should be removed from each layer?

Small architectures - Another research direction that is orthogonal to ours is to design smaller architectures that can be deployed on edge devices, such as SqueezeNet Iandola et al. (2016), MobileNet Sandler et al. (2018) and EfficientNet Tan & Le (2019). In this paper, our focus is to compress existing architectures while ensuring inference time speedups as well as maintaining prediction accuracy.

3 ADJOINED NETWORKS

In our training paradigm, the original (larger) and the smaller network are trained together. The motivation for this kind of training comes from the principle that *good teachers are lifelong learners*. Hence, the larger network which serves as a teacher for the smaller network should not be frozen (as in standard teacher-student architecture designs Hinton et al. (2015)). Rather both should learn together in a "combined learning environment", that is, adjoined networks. By learning together both the networks can be better together.

We are now ready to describe our approach and discuss the design of adjoined networks. Before that, let's take a re-look at the standard convolution operator. Let $\mathbf{x} \in \mathbf{R}^{h \times w \times c_{in}}$ be the input to a convolution layer with weights $\mathbf{W} \in \mathbf{R}^{c_{out} \times k \times k \times c_{in}}$ where c_{in}, c_{out} denotes the number of input and output channels, k the kernel size and h, w the height and width of the image. Then, the output of the convolution \mathbf{z} is given by

$$\mathbf{z} = conv(\mathbf{x}, \mathbf{W})$$

In the adjoined paradigm, a convolution layer with weight matrix \mathbf{W} and a binary mask matrix $M \in \{0, 1\}^{c_{out} \times k \times k \times c_{in}}$ receives two inputs \mathbf{x}_1 and \mathbf{x}_2 of size $h \times w \times c_{in}$ and outputs two vectors \mathbf{z}_1 and \mathbf{z}_2 as defined below.

$$\mathbf{z}_1 = conv(\mathbf{x}_1, \mathbf{W}) \quad \mathbf{z}_2 = conv(\mathbf{x}_2, \mathbf{W} * M) \quad (1)$$

Here M is of the same shape as \mathbf{W} and $*$ represents an element-wise multiplication. Note that the parameters of the matrix M are fixed before training and not learned. The vector \mathbf{x}_1 represents an input to the original (bigger) network while the vector \mathbf{x}_2 is the input to the smaller, compressed

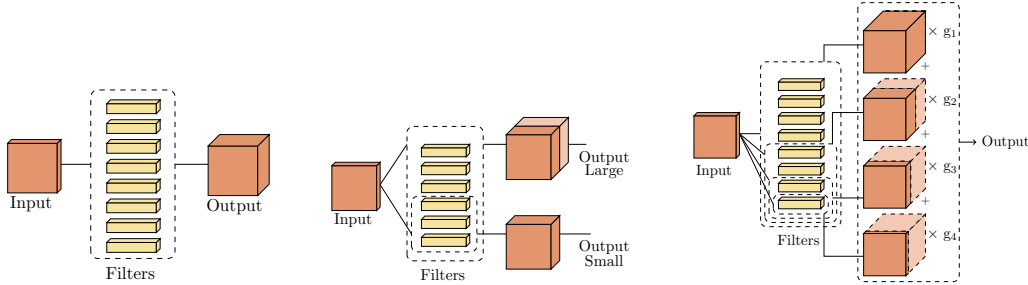


Figure 3: (Left) Standard layer of CNN. (Center) Layer in Adjoined Network. (Right) Layer in DAN.

network. For the first convolution layer of the network $\mathbf{x}_1 = \mathbf{x}_2$ but the two vectors are not necessarily equal for the deeper convolution layers (Fig. 2). The mask matrix M serves to zero-out some of the parameters of the convolution layer thereby enabling network compression. In this paper, we consider matrices M of the following form.

$$M := a_\alpha = \text{matrix such that the first } \frac{c_{out}}{\alpha} \text{ rows are all 1 and the rest 0} \quad (2)$$

In Section 7, we run experiments with $M := a_\alpha$ for $\alpha \in \{2, 4, 8, 16\}$. Putting this all together, we see that any CNN-based architecture can be converted and trained in an adjoined fashion by replacing the standard convolution operation by the adjoined convolution operation (Eqn. 1). Since the first layer receives a single input (Fig. 2), two copies are created which are passed to the adjoined network. The network finally gives two outputs \mathbf{p} corresponding to the original (bigger or unmasked) network and \mathbf{q} corresponding to the smaller (compressed) network, where each convolution operation is done using a subset of the parameters described by the mask matrix M (or M_α). We train the network using a novel time-dependent loss function which forces \mathbf{p} and \mathbf{q} to be close to one another (Defn. 1).

4 ONE-SHOT REGULARIZATION AND COMPRESSION

In the previous section, we looked at the design on adjoined networks. For one input $(\mathbf{X}, \mathbf{y}) \in \mathbf{R}^{h \times w \times c_{in}} \times [0, 1]^{n_c}$, the network outputs two vectors \mathbf{p} and $\mathbf{q} \in [0, 1]^{n_c}$ where n_c denotes the number of classes and c_{in} denotes the number of input channels (equals 3 for RGB images).

Definition 1 (Adjoined loss). *Let \mathbf{y} be the ground-truth one-hot encoded vector and \mathbf{p} and \mathbf{q} be output probabilities by the adjoined network. Then*

$$\mathcal{L}(\mathbf{y}, \mathbf{p}, \mathbf{q}) = -\mathbf{y} \log \mathbf{p} + \lambda(t) KL(\mathbf{p}, \mathbf{q}) \quad (3)$$

where $KL(\mathbf{p}, \mathbf{q}) = \sum_i p_i \log \frac{p_i}{q_i}$ is the measure of difference between two probability measures Kullback & Leibler (1951). The regularization term $\lambda : [0, 1] \rightarrow \mathbf{R}$ is a function which changes with the number of epochs during training. Here $t = \frac{\text{current epoch}}{\text{Total number of epochs}}$ equals zero at the start of training and equals one at the end.

In our definition of the loss function, the first term is the standard cross-entropy loss function which trains the bigger network. To train the smaller network, we use the predictions from the bigger network as a soft ground-truth signal. We use KL-divergence to measure how far the output of the smaller network is from the bigger network. This also has a regularizing effect as it forces the network to learn from a smaller set of parameters. Note that, in our implementations, we use $KL(\mathbf{p}, \mathbf{q}) = \sum p_i \log \frac{p_i + \epsilon}{q_i + \epsilon}$ to avoid rounding and division by zero errors where $\epsilon = 10^{-6}$.

At the start of training, \mathbf{p} is not a reliable indicator of the ground-truth labels. To compensate for this, the regularization term λ changes with time. In our experiments, we used $\lambda(t) = \min\{4t^2, 1\}$. Thus, the contribution of the second term in the loss is zero at the beginning and steadily grows to one at 50% training. We experiment with different choices of the regularization function λ the results of which are in the appendix .

5 DAN: DIFFERENTIABLE ADJOINED NETWORKS

In Sections 3 and 4, we described the framework of adjoined networks and the corresponding loss function. An important parameter in the design of these networks is the choice of parameter α . For example, using a value of $\alpha = 2$ corresponds to ‘selecting’ only half of the filters from each convolution layer. Note that the choice of α is global. However, choosing α independently for each layer would add more flexibility to the current framework. To solve this problem, we propose the framework of Differentiable Adjoined Networks (or DAN).

Consider the following example of a network with 50 convolution layers with the following choices for $\alpha \in A = \{1, 2, 4, 8, 16\}$. Finding the optimal network structure involves searching over a space of size 5^{50} . DAN encodes architectures as a weight sharing a super-net and optimizes the weights to find the best architecture (Fig 3).

Let $\mathbf{x} \in R^{h \times w \times c_{in}}$ be the input to a convolution layer with weights $W \in R^{c_{out} \times k \times k \times c_{in}}$ where c_{in}, c_{out} denotes the number of input and output channels, k the kernel size and h, w the height and width of the image. Let $A = \{\alpha_1, \dots, \alpha_p\}$ be the range of values of α for the layer. Then, the output \mathbf{z} of the DAN convolution layer is given by

$$z = \sum_{i=1}^p g_i z_i \quad (4)$$

Here z_i represents the output of the i^{th} adjoined convolution layer given by $z_i = \text{conv}(\mathbf{x}, W * M_i)$ where M_i is the mask matrix corresponding to α_i (as in Eqn. 2). g_i ’s also referred to as Gumbel weights are given by

$$g_i = \frac{\exp[\eta_i + \epsilon_i]/\tau}{\sum_i \exp[(\eta_i + \epsilon_i)/\tau]} \quad (5)$$

Here η_i is a learnable parameter, τ is called temperature and controls the rate of decay, and $\epsilon_i \sim N(0, 1)$ is uniform random noise (also referred to as gumbel noise). The idea of combining multiple outputs using gumbel weights has previously been employed successfully in architecture search Wan et al. (2020). Next, we define our loss function.

Definition 2 (Differentiable Adjoined loss). *Let y be the ground-truth one-hot encoded vector and p and q be output probabilities by the adjoined network n_f represent the FLOPs of the smaller network. Then*

$$\mathcal{L}(y, p, q, n_f) = -y \log p + \lambda(t)(KL(p, q) + \gamma n_f) \quad (6)$$

where $KL(p, q)$, $\lambda(t)$ are same as used in Eqn. 1. n_f represents total floating point operations or FLOPs of the network. γ is a constant.

Differentiable Adjoined Loss is similar to Adjoined Loss defined in Def 1. It has three terms, cross-entropy to train the bigger network, KL div to minimize the distance between the bigger and smaller network, and latency term to minimize the FLOPs of the searched architecture. In DAN the output is a weighted sum of multiple networks. While training, temperature (τ) in gumbel softmax is decreased. As τ approaches zero, gumbel weights approximates to a one-hot vector. After training, at each layer, α fraction corresponding to the max gumbel weight is chosen. The architecture found using DAN is then trained normally in adjoined fashion to get trained weights of the compressed model.

6 THEORY: REGULARIZATION BEHAVIOR

To study the regularization behavior of adjoined training paradigm (or the loss function), we consider the following neural network model. A multi-layer neural network that has only convolution or linear fully-connected layers with two possible choices for activation function, ReLU or the linear function. Although neural networks used in practice often have other types of layers like max-pooling, batch-normalization etc. and other possible activation functions, the proposed model is often studied as a first step towards understanding the dynamics and behavior of deep networks (for example in Phuong & Lampert (2019), Saxe et al. (2013), Kawaguchi (2016) and Hardt & Ma (2016)). We are now ready to state the main theoretical result of this paper.

Theorem 6.1. Given a deep neural network \mathcal{A} which consists of only convolution and linear layers. Let the network use one of $f(x) = \min\{x, 0\}$ (relu) or $f(x) = x$ (linear) as the activation function. Let the network be trained using the adjoined loss function as defined in Eqn. 3. Let \mathbf{X} be the set of parameters of the network \mathcal{A} which is shared across both the smaller and bigger networks. Let \mathbf{Y} be the set of parameters of the bigger network not shared with the smaller network. Let \mathbf{p} be the output of the larger network and let \mathbf{q} be the output of the smaller network where $\mathbf{p}_i, \mathbf{q}_i$ represents their i^{th} component. Then, the adjoined loss function induces a data-dependent regularizer with the following properties.

- For all $x \in X$, the induced L_2 penalty is given by $\sum_i \mathbf{p}_i (\log' \mathbf{p}_i - \log' \mathbf{q}_i)^2$
- For all $y \in Y$, the induced L_2 penalty is given by $\sum_i \mathbf{p}_i (\log' \mathbf{p}_i)^2$

Proof sketch To analyze the induced L_2 penalty, we consider the second order Taylor approximation of the KL-divergence term for all parameters $x \in \mathbf{X}$ and for all $y \in \mathbf{Y}$. By treating, p_i (and q_i) as functions of the given parameter x (or y) and careful analysis gives us the result of the theorem. The detailed derivations are in the appendix . \square

Thm. 6.1 shows that for that shared parameters x , adjoined loss penalizes those parameters whose rate of change between the larger and smaller networks is large (on the log scale). Hence, it encourages' parameters that have similar behavior (rate of change) on both the networks. Similarly, for the over-parameterized weights of the model y , the regularization imposed by the adjoined loss is such that if these parameters change a lot (on the log scale) then the penalty imposed on such parameters is more. Thus, adjoined loss "encourages" such parameters to not change by a lot thereby enabling compression.

7 EXPERIMENTS

We are now ready to describe our experiments in detail. We run experiments on two different datasets. (1) *ImageNet* - an image classification dataset Russakovsky et al. (2015) with 1000 classes and about 1.2M images . (2) *CIFAR-100* - a collection of 60k images in 100 classes Krizhevsky et al. (2009). For both of these datasets, we use standard data augmentation techniques like random-resize cropping, random flipping etc. The details are provided in the appendix .

We train different architectures on all of the above datasets. Namely, ResNet-100, ResNet-50, ResNet-18 and DenseNet-121. The detailed architecture diagram can be found in appendix . On each dataset, we first train these architectures in the standard non-adjoined fashion using the cross-entropy loss function. We will refer to it by the name *Standard*. Next, we train the adjoined network, obtained by replacing the standard convolution operation with the adjoined convolution operation, using the adjoined loss function. In the second step, we obtain two different networks. In this section, we refer to them by *AN-X-Full* and the *AN-X-Small* networks where X represents the number of layers. For eg. *AN-50-Full*, *AN-50-Small* represents larger and smaller networks obtained on adjoinedly training ResNet-50. *AN-121-Full*, *AN-121-Small* represents models obtained on adjoinedly training DenseNet-121. We compare the performance of the AN-X-Full and AN-X-Small networks against the standard network. One point to note is that we do not replace the convolutions in the stem layers but only those in the res-blocks. Since most of the weights are in the later layers, this leads to significant space and time savings while retaining competitive accuracy. DAN describes the performace of adjoined network on architectures found by Differentiable Adjoined Network. DAN-50 has the same number of blocks as ResNet-50 whereas DAN-100 has twice the number of blocks of ResNet-50. More details regarding the architecture can be found in the appendix .

We ran our experiments on GPU enabled machine using Pytorch, hyperparameters for the experiments are mentioned in the supplementary. We have also open-sourced our implementation ¹.

In Section 7.1, we compare our compression results against other structured pruning methods. In Section 7.2, we compare AN with various types of knowledge distillation methods. In Section 7.3, we describe our results for compression and performance of architectures found by DAN. In Section 7.4, we show the strong regularizing effect of AN training. The detailed results are included in the appendix .

¹The code can be found at <https://github.com/utkarshnath/Adjoint-Network.git>

7.1 COMPARISON AGAINST OTHER STRUCTURED PRUNING WORKS

Model Compression Results				
Method	# Params	GFLOPs	Accuracy	Reference
ABCPruner-0.8	11.75	1.89	73.86	Lin et al. (2020b)
ABCPruner-0.7	11.24	1.8	73.52	Lin et al. (2020b)
GBN-50	11.91	1.9	75.18	You et al. (2019)
GBN-60	17.6	2.43	76.19	You et al. (2019)
DCP	12.3	1.82	74.95	Zhuang et al. (2018)
HRank	16.15	2.3	74.98	Lin et al. (2020a)
HRank	13.77	1.55	71.98	Lin et al. (2020a)
HRank	8.27	0.98	69.1	Lin et al. (2020a)
MetaPruning	19.1	2	75.4	Liu et al. (2019b)
MetaPruning	12.7	1	73.4	Liu et al. (2019b)
Slimmable Net	19.2	2.3	74.9	Yu et al. (2018)
Slimmable Net	12.8	1.1	72.1	Yu et al. (2018)
AN-50-Small a_4 (our)	2.2	1.6	71.82	
DAN-50 (our)	3.49	1.7	73.33	
DAN-100 (our)	6.58	2.15	75.43	
AN-50-Small a_2 (our)	7.14	2.2	75.1	

Table 1: The table shows the performance of various structured pruning methods when trained on the ImageNet dataset. a_α in AN-50-Small denotes the mask matrix as defined in Eqn. 2.

Table 1 and Figure 1 compares the performance of various structured compression schemes on the ImageNet dataset for the ResNet-50 architecture. Note, these methods provide inference speed-up without special hardware or software. We see that the adjoined training regime can achieve compression that is significantly better than other methods considered in the literature. In Figure 1, models trained using our paradigm are explicitly on the left side of the graph while other methods are clustered on to the right side. Other methods obtain compression ratios in the range $2 - 3 \times$, compared to which our method achieves up to $12 \times$ compression in size. Similarly, GFLOPS for our method is amongst the highest as compared to the other state-of-the-art works, while suffering a small accuracy drop as compared against the base ResNet-50 model.

7.2 COMPARISON AGAINST OTHER KNOWLEDGE DISTILLATION WORKS

Knowledge Distillation Variants						
Network	AN (Our)	KD	RKD	VID	FT	CC
AN-50-Small a_2	76.9	75.8	76.76	76.33	76	76.4
AN-50-Small a_4	75.38	74.32	75.03	74.6	71.07	75.01
AN-50-Small a_8	74.63	72.89	73.6	73.5	66.2	72.8
AN-50-Small a_{16}	72.1	70.6	70.9	70.8	64.63	70.1

Table 2: AN compared to various state-of-the-art KD methods – KD (Hinton et al. (2015)), RKD (Park et al. (2019)), VID (Ahn et al. (2019)), FT (Kim et al. (2020)) and CC (Peng et al. (2019)). a_α is same as in Table 1.

In this section, we discuss the effectiveness of weight sharing and training two networks together. We compare AN against the various state-of-the-art variants of knowledge distillation. In Table 2 and Figure 4, we compare accuracy (Top-1%) of AN-50-Small against the same architecture trained using various KD variants on CIFAR-100 dataset. Pre-trained ResNet-50 was used as the teacher model for KD variants. ResNet-50 was trained on CIFAR-100 using standard training paradigm. We see that the model trained using AN significantly outperforms the models trained using various teacher-student paradigm showing the effectiveness of training a subset of weights together.

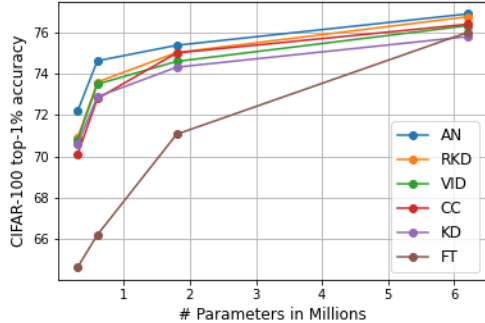


Figure 4: Adjoined Network compared to various state-of-the-art KD methods.

Compression using AN paradigm					
Dataset	Network	Hyperparameter	# Params (M)	GFLOPs	Accuracy
CIFAR-100	ResNet-50		23.7	0.338	76.8
	AN-50-Small	a_2	6.15	0.140	76.9
	AN-50-Small	a_8	0.67	0.074	74.63
	DAN-50	1, 2, 4, 8, 16	1.64	0.084	75.1
	DAN-100	1, 2, 4	6.7	0.173	77.62
	ResNet-18		11.26	0.153	74.37
	AN-18-Small	a_4	0.91	0.059	71.61
	DenseNet-121		6.96	0.888	79.0
	AN-121-Small	a_2	1.77	0.502	78.3
	AN-121-Small	a_4	0.7	0.411	76.38
ImageNet	ResNet-100		46.99	8.47	77.3
	AN-100-Small	a_4	3.86	2.68	74.51
	ResNet-50		25.5	4.7	76.1
	AN-50-Small	a_2	7.14	2.2	75.1
	AN-50-Small	a_4	2.2	1.6	71.84
	DAN-50	2, 4	3.49	1.74	73.33
	DAN-100	2, 4, 8	5.22	1.85	74.78
	DAN-100	4, 8	6.58	2.15	75.43
	DAN-100	1, 2, 4	12.5	2.95	75.71

Table 3: For AN, hyperparameter a_α denote the masking matrix (defined in Eqn. 2), For DAN it denotes the search space. Detailed results can be found in the appendix .

7.3 ABLATION STUDY: COMPRESSION

Table 3 compares the performance (top 1% accuracy) of the models compressed using Adjoined training paradigm against the performance of standard network. For AN, we use the a_α as the masking matrix (defined in Eqn. 2). The mask is such that the last $(1 - \frac{1}{\alpha})$ filters are zero. Hence, these can be pruned away to support fast inference. We also observe that ResNet-50 is a bigger network and can be compressed more. Also, different datasets can be compressed by different amounts. For example, on CIFAR-100 dataset, the network can be compressed by factors $\sim 35\times$ while for other datasets it ranges from $2\times$ to $12\times$. DAN is able to search compressed architecture with minimum loss in accuracy as compared to base architecture. For ImageNet, DAN architectures were searched on Imagewoof (a proxy dataset with 10 different dog breeds from ImageNet Howard (2019); Shleifer & Prokop (2019)). γ as defined in Def. 2 is e^{-13} , e^{-19} for DAN-50 and DAN-100 respectively. During architecture search, temperature τ in gumbel softmax was initialized to 15 and exponentially annealed by $e^{-0.045}$ every epoch.

7.4 ABLATION STUDY: REGULARIZATION

Table 4 compares the performance of the base network trained in adjoined fashion (AN-Full) to the same network trained in Standard fashion. We see a consistent trend that the network trained adjoinedly outperforms the same network trained in the standard way. We see maximum gains on CIFAR-100, exceeding accuracy by as much as 1.8%. Even on ImageNet, we see a gain of about 0.77%.

8 CONCLUSION

In this work, we introduced the paradigm of Adjoined Network training where both the larger teacher (or base) network and the smaller student network are trained together. We showed how this approach to training neural networks can allow us to reduce the number of parameters of large networks like ResNet-50 by $12\times$, (even going up to $35\times$ on some datasets) without significant loss in classification accuracy with $2-3\times$ reduction in the number of FLOPs. We showed (both theoretically and experimentally) that adjoining a large and a small network together

AN-Full vs Standard			
Network	α	AN-Full	Standard
CIFAR-100			
ResNet-50	a_8	77.36	76.8
ResNet-18	a_2	74.8	74.3
DenseNet-121	a_4	80.8	79.0
ImageNet			
ResNet-50	a_2	76.87	76.1
ResNet-50	a_4	75.84	76.1

Table 4: a_α is same as in Table 3. Detailed results can be found in the appendix .

has a regularizing effect on the larger network. We also introduced DAN, a search strategy that automatically selects the best architecture for the smaller student network. Augmenting adjoined training with DAN, the smaller network achieves accuracy that is close to that of the base teacher network (even surpassing the base network on some datasets like CIFAR-100).

REFERENCES

Sungsoo Ahn, Shell Xu Hu, Andreas Damianou, Neil D. Lawrence, and Zhenwen Dai. Variational information distillation for knowledge transfer, 2019.

Han Cai, Ligeng Zhu, and Song Han. Proxylessnas: Direct neural architecture search on target task and hardware, 2019.

Utku Evci, Trevor Gale, Jacob Menick, Pablo Samuel Castro, and Erich Elsen. Rigging the lottery: Making all tickets winners, 2021.

Trevor Gale, Erich Elsen, and Sara Hooker. The state of sparsity in deep neural networks, 2019.

Song Han, Huizi Mao, and William J Dally. Deep compression: Compressing deep neural networks with pruning, trained quantization and huffman coding. *arXiv preprint arXiv:1510.00149*, 2015.

Song Han, Xingyu Liu, Huizi Mao, Jing Pu, Ardavan Pedram, Mark A. Horowitz, and William J. Dally. Eie: Efficient inference engine on compressed deep neural network, 2016.

Moritz Hardt and Tengyu Ma. Identity matters in deep learning. *arXiv preprint arXiv:1611.04231*, 2016.

Geoffrey Hinton, Oriol Vinyals, and Jeff Dean. Distilling the knowledge in a neural network. *arXiv preprint arXiv:1503.02531*, 2015.

Jeremy Howard. Imagenette. URL: *Github repository with links to dataset*. <https://github.com/fastai/imagenette>, 2019.

Forrest N Iandola, Song Han, Matthew W Moskewicz, Khalid Ashraf, William J Dally, and Kurt Keutzer. SqueezeNet: Alexnet-level accuracy with 50x fewer parameters and < 0.5 mb model size. *arXiv preprint arXiv:1602.07360*, 2016.

Kenji Kawaguchi. Deep learning without poor local minima. In *Advances in neural information processing systems*, pp. 586–594, 2016.

Jangho Kim, SeongUk Park, and Nojun Kwak. Paraphrasing complex network: Network compression via factor transfer, 2020.

Alex Krizhevsky, Vinod Nair, and Geoffrey Hinton. Cifar-10 and cifar-100 datasets. URL: <https://www.cs.toronto.edu/kriz/cifar.html>, 6, 2009.

Solomon Kullback and Richard A Leibler. On information and sufficiency. *The annals of mathematical statistics*, 22(1):79–86, 1951.

Aditya Kusupati, Vivek Ramanujan, Raghav Soman, Mitchell Wortsman, Prateek Jain, Sham Kakade, and Ali Farhadi. Soft threshold weight reparameterization for learnable sparsity, 2020.

Hao Li, Asim Kadav, Igor Durdanovic, Hanan Samet, and Hans Peter Graf. Pruning filters for efficient convnets. *arXiv preprint arXiv:1608.08710*, 2016.

Mingbao Lin, Rongrong Ji, Yan Wang, Yichen Zhang, Baochang Zhang, Yonghong Tian, and Ling Shao. Hrank: Filter pruning using high-rank feature map. In *Proceedings of the IEEE/CVF Conference on Computer Vision and Pattern Recognition*, pp. 1529–1538, 2020a.

Mingbao Lin, Rongrong Ji, Yuxin Zhang, Baochang Zhang, Yongjian Wu, and Yonghong Tian. Channel pruning via automatic structure search. *arXiv preprint arXiv:2001.08565*, 2020b.

Hanxiao Liu, Karen Simonyan, and Yiming Yang. Darts: Differentiable architecture search, 2019a.

Zechun Liu, Haoyuan Mu, Xiangyu Zhang, Zichao Guo, Xin Yang, Tim Kwang-Ting Cheng, and Jian Sun. Metapruning: Meta learning for automatic neural network channel pruning, 2019b.

Zhuang Liu, Jianguo Li, Zhiqiang Shen, Gao Huang, Shoumeng Yan, and Changshui Zhang. Learning efficient convolutional networks through network slimming. In *Proceedings of the IEEE International Conference on Computer Vision*, pp. 2736–2744, 2017.

Jongsoo Park, Sheng Li, Wei Wen, Ping Tak Peter Tang, Hai Li, Yiran Chen, and Pradeep Dubey. Faster cnns with direct sparse convolutions and guided pruning, 2017.

Wonpyo Park, Dongju Kim, Yan Lu, and Minsu Cho. Relational knowledge distillation, 2019.

Baoyun Peng, Xiao Jin, Jiaheng Liu, Shunfeng Zhou, Yichao Wu, Yu Liu, Dongsheng Li, and Zhaoning Zhang. Correlation congruence for knowledge distillation, 2019.

Mary Phuong and Christoph Lampert. Towards understanding knowledge distillation. In *International Conference on Machine Learning*, pp. 5142–5151, 2019.

Esteban Real, Sherry Moore, Andrew Selle, Saurabh Saxena, Yutaka Leon Suematsu, Jie Tan, Quoc Le, and Alex Kurakin. Large-scale evolution of image classifiers, 2017.

Adriana Romero, Nicolas Ballas, Samira Ebrahimi Kahou, Antoine Chassang, Carlo Gatta, and Yoshua Bengio. Fitnets: Hints for thin deep nets, 2015.

Olga Russakovsky, Jia Deng, Hao Su, Jonathan Krause, Sanjeev Satheesh, Sean Ma, Zhiheng Huang, Andrej Karpathy, Aditya Khosla, Michael Bernstein, Alexander C. Berg, and Li Fei-Fei. ImageNet Large Scale Visual Recognition Challenge. *International Journal of Computer Vision (IJCV)*, 115 (3):211–252, 2015. doi: 10.1007/s11263-015-0816-y.

Mark Sandler, Andrew Howard, Menglong Zhu, Andrey Zhmoginov, and Liang-Chieh Chen. Mobilenetv2: Inverted residuals and linear bottlenecks. In *Proceedings of the IEEE conference on computer vision and pattern recognition*, pp. 4510–4520, 2018.

Andrew M Saxe, James L McClelland, and Surya Ganguli. Exact solutions to the nonlinear dynamics of learning in deep linear neural networks. *arXiv preprint arXiv:1312.6120*, 2013.

Sam Shleifer and Eric Prokop. Using small proxy datasets to accelerate hyperparameter search. *arXiv preprint arXiv:1906.04887*, 2019.

Mingxing Tan and Quoc V Le. Efficientnet: Rethinking model scaling for convolutional neural networks. *arXiv preprint arXiv:1905.11946*, 2019.

Mingxing Tan, Bo Chen, Ruoming Pang, Vijay Vasudevan, Mark Sandler, Andrew Howard, and Quoc V. Le. Mnasnet: Platform-aware neural architecture search for mobile, 2019.

Alvin Wan, Xiaoliang Dai, Peizhao Zhang, Zijian He, Yuandong Tian, Saining Xie, Bichen Wu, Matthew Yu, Tao Xu, Kan Chen, Peter Vajda, and Joseph E. Gonzalez. Fbnetv2: Differentiable neural architecture search for spatial and channel dimensions. In *CVPR*, pp. 12962–12971. IEEE, 2020.

Bichen Wu, Xiaoliang Dai, Peizhao Zhang, Yanghan Wang, Fei Sun, Yiming Wu, Yuandong Tian, Peter Vajda, Yangqing Jia, and Kurt Keutzer. Fbnet: Hardware-aware efficient convnet design via differentiable neural architecture search, 2019.

Zhonghui You, Kun Yan, Jinmian Ye, Meng Ma, and Ping Wang. Gate decorator: Global filter pruning method for accelerating deep convolutional neural networks. *arXiv preprint arXiv:1909.08174*, 2019.

Jiahui Yu, Linjie Yang, Ning Xu, Jianchao Yang, and Thomas Huang. Slimmable neural networks. *arXiv preprint arXiv:1812.08928*, 2018.

Ying Zhang, Tao Xiang, Timothy M Hospedales, and Huchuan Lu. Deep mutual learning. In *Proceedings of the IEEE Conference on Computer Vision and Pattern Recognition*, pp. 4320–4328, 2018.

Michael Zhu and Suyog Gupta. To prune, or not to prune: exploring the efficacy of pruning for model compression, 2017.

Zhuangwei Zhuang, Mingkui Tan, Bohan Zhuang, Jing Liu, Yong Guo, Qingyao Wu, Junzhou Huang, and Jinhui Zhu. Discrimination-aware channel pruning for deep neural networks. *arXiv preprint arXiv:1810.11809*, 2018.

Barret Zoph and Quoc V. Le. Neural architecture search with reinforcement learning, 2017.

A REGULARIZATION THEORY

Theorem A.1. *Given a deep neural network \mathcal{A} which consists of only convolution and linear layers. Let the network use one of $f(x) = \min\{x, 0\}$ (relu) or $f(x) = x$ (linear) as the activation function. Let the network be trained using the adjoined loss function as defined in Eqn. 3. Let \mathbf{X} be the set of parameters of the network \mathcal{A} which is shared across both the smaller and bigger networks. Let \mathbf{Y} be the set of parameters of the bigger network not shared with the smaller network. Let \mathbf{p} be the output of the larger network and let \mathbf{q} be the output of the smaller network. Then, the adjoined loss function induces a data-dependent regularizer with the following properties.*

- For all $x \in X$, the induced L_2 penalty is given by $\sum_i \mathbf{p}_i (\log' \mathbf{p}_i - \log' \mathbf{q}_i)^2$
- For all $y \in Y$, the induced L_2 penalty is given by $\sum_i \mathbf{p}_i (\log' \mathbf{p}_i)^2$

Proof. We are interested in analyzing the regularizing behavior of the following loss function. $-y \log p + KL(p, q) y$ is the ground truth label, p is the output probability vector of the bigger network and q is the output probability vector of the smaller network. Recall that the parameters of smaller network are shared across both. We will look at the second order taylor expansion for the kl-divergence term. This will give us insights into regularization behavior of the loss function.

Let x be a parameter which is common across both the networks and y be a parameter in the bigger network but not the smaller one.

$$D(x) = \sum_i p_i(x) (\log p_i(x) - \log q_i(x)) \text{ and } D(y) = \sum_i p_i(y) (\log p_i(y) - \log q_i)$$

For the parameter y , q_i is a constant. Now, computing the first order derivative, we get that

$$\begin{aligned} D'(x) &= \sum_i p'_i(x) (\log p_i(x) - \log q_i(x)) + p'_i(x) - \frac{q'_i(x)p_i(x)}{q_i(x)} \\ D'(y) &= \sum_i p'_i(y) (\log p_i(y) - \log q_i) + p'_i(y) \end{aligned}$$

Now, computing the second derivative for both the types of parameters, we get that

$$\begin{aligned} D''(x) &= \sum_i p''_i(x) (\log p_i(x) - \log q_i(x)) + p'_i(x) \left(\frac{p'_i(x)}{p_i(x)} - \frac{q'_i(x)}{q_i(x)} \right) + p''_i(x) \\ &\quad - \frac{q_i(x)q'_i(x)p'_i(x) + q_i(x)q''_i(x)p_i(x) - q'_i(x)q'_i(x)p_i(x)}{q_i^2(x)} \\ D''(y) &= \sum_i p''_i(y) (\log p_i(y) - \log q_i) + \frac{p'_i(y)p'_i(y)}{p_i(y)} + p''_i(y) \\ D''(x) &= \sum_i \frac{p'_i(x)p'_i(x)}{p_i(x)} - \frac{2p'_i(x)q'_i(x)}{q_i(x)} + \frac{q'_i(x)q'_i(x)p_i(x)}{q_i^2(x)} \\ &= \sum_i p_i(x) \left(\frac{p'_i(x)}{p_i(x)} - \frac{q'_i(x)}{q_i(x)} \right)^2 = \sum_i p_i (\log' p_i - \log' q_i)^2 \end{aligned} \tag{7}$$

Similarly, for the parameters only in the bigger network, we get that

$$D''(y) = \sum_i \frac{p'_i(y)p'_i(y)}{p_i(y)} = \sum_i p_i (\log' p_i)^2 \quad (8)$$

Note that y represents the over-parameterized weights of the model. The equations above show that the regularization imposed by the KL-divergence term on these parameters is such that if these parameters change a lot (on the log scale) then the penalty imposed on such parameters is more. Thus, the kl-divergence term encourages such parameters not to change by a lot. \square

B DATA AUGMENTATION AND HYPERPARAMETERS

We use different data-augmentation techniques for different datasets. Below are the details.

- *CIFAR-100*

We apply the following set of transforms for these datasets. (1) We horizontal flip the image with probability 0.5. (2) We normalize the image by using the following mean [0.5071, 0.4867, 0.4408] and standard [0.2675, 0.2565, 0.2761].

- *ImageNet*

On these two datasets, we apply the following set of transforms. (1) Random resize cropping - Crop a rectangular region with aspect ratio in $[3/4, 4/3]$ (selected uniformly at random) with area in $[0.08, 1.0]$ of the original area. (2) Flip the image horizontally with probability 0.5. (3) Normalize the image by dividing all pixel values of 255.0.

For CIFAR-100, input size is 32×32 for all the other datasets, the input size is 224×224 . The above transforms are applicable for the training dataset. For validation, we use center crop - select the center of the image with 85% area, followed by a normalization step. Note that our data augmentation are not heavily optimized for accuracy. Rather our goal is to compare adjoined training with standard training. Hence, we use the same data augmentation steps for both the trainings. For standard training, our accuracies are still comparable to the accuracies reported in the literature on these datasets using the ResNet-18 and ResNet-50 architectures. However, the adjoined training methodology proposed in this paper outperforms the network trained in the standard way.

ImageNet was trained for 100 epochs using learning rate initially set to $4e - 3$. We used adam optimizer with a cosine learning rate schedule with gradual warm-up for training on ImageNet. For CIFAR-100 we used SGD optimizer for 240 epochs with $lr = 0.05$. MultiStepLR was used to decay the learning rate by 0.1 at 150, 180, 210th epoch.

More details of the data-augmentation, hyper-parameter settings can be found in the code provided with the supplementary materials.

C RESNET ARCHITECTURE DIAGRAM

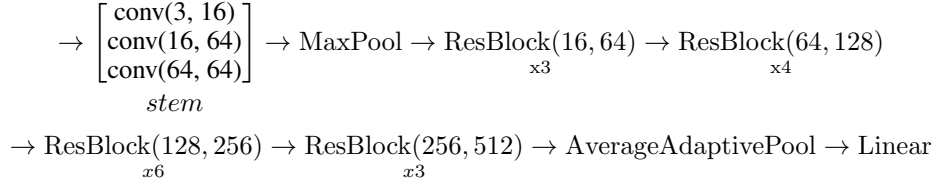


Figure 5: Architecture diagram for ResNet-50 network used in this paper. $conv(ni, no)$ is a combination of convolution layer with ni input and no output channels followed by a batch norm and relu layer. The ResBlocks are as defined in Fig. 6.

The architecture for ResNet-50 is depicted in Figs. 5 and 6. Each $conv$ layer is actually a combination of three layers. A standard convolution layer followed by a batch normalization layer followed by

$$\longrightarrow \begin{bmatrix} \text{conv}(4ni, no) \\ \text{conv}(no, no) \\ \text{conv}(no, 4no) \end{bmatrix} \longrightarrow \begin{bmatrix} \text{conv}(4no, no) \\ \text{conv}(no, no) \\ \text{conv}(no, 4no) \end{bmatrix} \\ x(l-1)$$

Figure 6: A ResBlock with l layers and input ni and output no .

a relu activation. The *ResBlock* refers to the residual blocks in ResNet architecture. Note that the skip connections are not shown in these diagrams. ResNet-100 is similar to ResNet-50 but instead of repeating blocks 3, 4, 6 and 3 times, blocks are repeated for 6, 8, 12 and 6 times. The same architecture has been used for searching in DAN-100. In ResNet-18 architecture, each resblock is repeated twice. Also, the resblock does not have a factor four in the convolution input and output.

For adjoined networks, the convolution parameters of all the last three resblocks are shared across both the original and the smaller architecture. Note that both the networks have different parameters for the batch-norm layers.

D DETAILED EXPERIMENTAL RESULTS

D.1 EXPERIMENTS ON CIFAR-100

Training with ResNet-50 on CIFAR-100					
Training paradigm	Masking matrix (M)	Top-1% Full	Top-1% Small	# Params (M)	FLOPs
Standard		76.8		23.7	338.59
AN	a_2	77.36	76.9	6.15	140.57
AN	a_4	76.8	75.38	1.8	88.94
AN	a_4	77.1	74.63	0.67	74.97
AN	a_{16}	76.8	72.1	0.38	70.95

Table 5: Accuracy for the various training paradigms for ResNet-50 trained on CIFAR-100. For AN training paradigm # Params and FLOPs represents number of parameters, FLOPs of the smaller model.

Training with ResNet-18 on CIFAR-100					
Training paradigm	Masking matrix (M)	Top-1% Full	Top-1% Small	# Params (M)	FLOPs
Standard		74.37		11.26	153.89
AN	a_2	74.8	73.62	3.00	78.62
AN	a_4	74	71.61	0.91	59.47
AN	a_8	74	68	0.39	54.29

Table 6: Accuracy for the various training paradigms for ResNet-18 trained on CIFAR-100. For AN training paradigm # Params and FLOPs represents number of parameters (in millions), FLOPs of the smaller model.

Training with DenseNet-121 on CIFAR-100					
Training paradigm	Masking matrix (M)	Top-1% Full	Top-1% Small	# Params (M)	FLOPs
Standard		79		6.96	888
AN	a_2	80.76	78.3	1.77	502
AN	a_4	80.8	76.38	0.7	411
AN	a_8	79	72.13	0.46	387

Table 7: Accuracy for the various training paradigms for ResNet-18 trained on CIFAR-100. For AN training paradigm # Params and FLOPs represents number of parameters (in millions), FLOPs of the smaller model.

D.2 EXPERIMENTS ON IMAGENET

Training with ResNet-50 on ImageNet					
Training paradigm	Masking matrix (M)	Top-1% Full	Top-1% Small	# Params (M)	GFLOPs
Standard		76.1		25.5	4.7
AN	a_2	76.87	75.1	7.1	2.2
AN	a_4	75.84	71.84	2.2	1.6
AN	a_8	73.46	64.7	0.67	1.4

Table 8: Accuracy for the various training paradigms for ResNet-50 trained on ImageNet. For AN training paradigm # Params and FLOPs represents number of parameters (in millions), FLOPs of the smaller model.

E CHOOSING THE REGULARIZATION FUNCTION

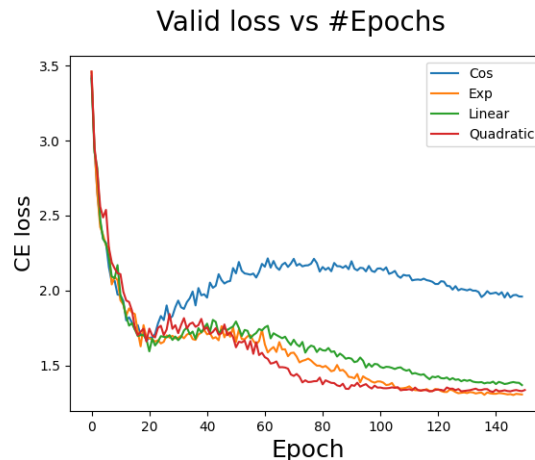


Figure 7: Validation cross entropy loss for various regularization functions. The networks were trained using AN a_4 mask matrix on CIFAR-100 using ResNet-18.

adjoined trained with different regularization functions		
Regularization function $\lambda(t)$	Top-1 Full	Top-1 Small
$1 - \cos(t)$	-2.86	-3.14
t	-0.1	-0.15
$\min\{4t^2, 1\}$	0.00	0.00
$\exp(t) - 1$	-0.37	+0.38

Table 9: The effect of training with different regularization functions on the top-1 accuracies of the bigger and the smaller networks. The quadratic function $\min\{4t^2, 1\}$ is used as the base for comparison.

Finally, we compare different choices of regularization function for the adjoined loss (Eqn. 3). For all the previous experiments, we use the ‘quadratic’ function $\lambda(t) = \min\{4t^2, 1\}$. In this section, we fix the architecture, dataset and mask matrix as ResNet-18, CIFAR-100 and a_4 respectively and vary the regularization function. We look at different functions which includes exponential and trigonometric functions. Table 9 and Fig. 7 both show the same trend. The cos function performs the worst while the rest have similar performance. We conjecture that any function that is close to zero for $t \leftarrow 0$ and grows to one eventually should be a reasonable choice for the regularization function. Note that throughout our discussion, we have used $\lambda(t) = c \min\{4t^2, 1\}$ with $c = 1$. Depending on the dataset, other values of c maybe more appropriate.